Insight into the Water Rock Interaction Process and Purification Mechanism of Mine Water in Underground Reservoir of Daliuta Coal Mine in China

Binbin Jiang
China University of Mining and Technology - Beijing Campus
Ju Gao
China University of Mining and Technology - Beijing Campus
Kun Du
China University of Mining and Technology - Beijing Campus
Xu Deng
China University of Mining and Technology - Beijing Campus
Kai Zhang (zhangkai@cumtb.edu.cn)
China University of Mining and Technology - Beijing Campus https://orcid.org/0000-0001-7735-7663

Research Article

Keywords: coal mine underground reservoir, mine water, rock characteristics, water rock interaction, water purification, PHREEQC

Posted Date: July 30th, 2021

DOI: https://doi.org/10.21203/rs.3.rs-665440/v1

Version of Record: A version of this preprint was published at Environmental Science and Pollution Research on January 6th, 2022. See the published version at https://doi.org/10.1007/s11356-021-18161-3.

Abstract

The process of water rock interaction and the purification mechanism of mine water quality were not clear after being stored in underground reservoir. This study based on the analysis of the hydrochemical characteristics of the reservoir water samples and the characterization of the rock samples, combined with PHREEQC analysis, the mechanism of water quality purification of mine water was discussed. The results showed that the rocks in the underground reservoir had layered silicate structure and flaky kaolinite structure, with some irregular edges and micro cracks, and higher specific surface area and total pore volume. These characteristics made the rocks had a certain adsorption and removal capacity for heavy metal ions and other pollutants in the mine water. The water rock interaction, such as the dissolution of albite and halite, the precipitation of gypsum and kaolinite, and the cation exchange, resulted in the increase of the concentration of Na^+ and the decrease of the concentration of Ca^{2+}, Mg^{2+} and TDS in the outlet water. This study also showed that PHREEQC analysis can be used to analyze the water rock interaction of coal mine underground reservoir and obtained more detailed information.

1. Introduction

The severe shortage of water has seriously hindered the development of the energy industry in many coal-producing areas (Chen et al., 2016; Rathi et al., 2017), especially in the Shendong Mining Area (Ma et al., 2013), located in the arid and semi-arid areas of northwest China but with rich coal reserves (Chen, 2016). The protection and rational utilization of water resources have become an important scientific and technological problem to be solved by coal green mining in arid areas of Northwest China (Zhang et al., 2011). In view of the above problems, Gu (Gu, 2015) put forward and successfully developed the coal mine underground reservoir technology using the cavity between the broken rock bodies in the mined space area formed after coal mining (Shi, 2021). The technology solves both the mine water disaster problem and realizes the efficient recycling of the mine water resources (Gu et al., 2016), providing more than 95% of the water use (Chen et al., 2016), which largely solves the production and domestic water problem in the mining area. During the operation of the underground reservoir in the coal mine, the collapsed rocks in the reservoir have a purification effect on the mine water (Gu et al., 2021), and scholars have also studied the purification effect of the rocks in the mined space area on the suspended matter, chemical oxygen demand (COD) (Fang, 2020), dissolved organic matter (DOM) (Han et al., 2020b; Yu et al., 2018) and heavy metals (Jiang et al., 2020; Shao, 2009) and so on. However, the purification mechanism of mine water in the process of water rock interaction between mine water and rock in reservoir storage stage is not clear.

The water rock interaction in the study area is closely related to the actual situation of the site (Jannesar Malakooti et al., 2015), so researchers usually use the field investigation sampling (Ibrahim et al., 2019) and indoor simulation experimental data (Goren et al., 2011; Phan et al., 2018), combined with the ion ratio method (Jia et al., 2020) or hydrogeochemical simulation software to accurately describe the physical and chemical relationship between the water phase composition and the regional environmental background, thus exploring the evolution and migration laws between the water and rock in the stratum (Kumar et al., 2020; Li et al., 2018). At present, some scholars (Han et al., 2020a) have analyzed the hydrochemical characteristics and formation mechanism of underground reservoir by testing the in-situ inflow and outflow water sample data of underground reservoir, combining multivariate statistical method, hydrochemical analysis method and ion ratio method. Some scholars (Fang et al., 2020) have studied the mechanism of water rock interaction and the source of ions in the underground reservoir from the change law of main ions (Zhang et al., 2019) and the characteristics of rock changes (Pearce et al., 2018; Zhang et al., 2020) through static simulation test of water rock interaction. The influence of water rock interaction on the binding characteristics of dissolved organic matter and heavy metals in mine water during the process of mine water flowing in goaf was also studied (Zhang et al., 2021). It can be seen that some achievements have been made in the study of water rock interaction in underground reservoir of coal mine, but there is no study of water rock interaction in reservoir combined with hydrogeochemical simulation.

Reverse geochemical simulation (Dai and Samper, 2006; Embile et al., 2019) is to determine the water rock reaction in the system based on the observed hydrochemical data, that is, to interpret the observed hydrochemical data. The purpose is to find out the complex reaction between groundwater and different minerals and gases, and quantify it under reasonable conditions (Hidalgo and Cruz-Sanjulián, 2001). With the rapid development of computer technology, many hydrogeochemical simulation software appeared (Salcedo Sánchez et al., 2017). Among them, PHREEQC has the most powerful simulation ability among the similar software (Sprocati et al., 2019). It has a huge database of groundwater balance model and ion exchange model (Steding et al., 2020), which can simulate the chemical reaction and migration process of sewage and clean water in the environment, and is widely used in the world (Mahani et al., 2016). In addition, scholars (Chandrasekhar et al., 2018; Korrani et al., 2015) have also conducted a lot of simulation studies on groundwater hydrochemical evolution and water rock interaction in artificial recharge process by using PHREEQC (Sharma and Mohanty, 2018), and the water rock interaction analysis software has been relatively mature (Shabani and Zivar, 2020).

In this study, Daliuta coal mine underground reservoir inlet and outlet water and roof caving rock samples were taken as the research object. Based on the analysis of mineral chemical composition, specific surface area and pore structure of roof caving rock samples and suspended solids in mine water in the study area, as well as the test and analysis of in-situ inflow and outflow water samples of underground reservoir, combined with the reverse geochemical simulation analysis was carried out with PHREEQC software. This paper reveals the process of water rock interaction in coal mine underground reservoir and the purification mechanism of mine water quality, which provides theoretical support and reference for the future application of PHREEQC software to simulate the process of water rock interaction in coal mine underground reservoir and the efficient utilization of reservoir water.

2 Study Area

The mine field area of Daliuta Coal Mine is 189.9 km^2, which is located in the northwest of Shenmu County, Yulin City, Shaanxi Province. The geographical coordinates are 39°13'53"N-39°21'32"N and 110°12'23"E-110°22'54"E. The mining area (Chen, 2016) is a hilly, forest, grassland to desert, Gannan grassland transition zone, belongs to the desert grass beach area, close to the semi-desert nature, and the natural vegetation is very few.

The average annual precipitation in Daliuta Mine(Wang et al., 2018) is 194.7 ~ 531.6 mm, which is the indirect water source in the mining area. On the surface of the mine, there are two great gullies, the Wu Lan Mulun River and the Niuchuan River, and some small water bodies, but the water quantity is limited and easy to be released, which does not affect the safety of mine production. The aquifer water contains bulk layer water, bedrock fissure water and caustic rock water. Due to the influence of mining failure in the mining area, the aquifer is rich in water and the overall recharge water is relatively limited. The data show that the unit water inflow of the Quaternary loose aquifer and Yan'an formation bedrock aquifer is 0.0026 ~ 0.6789 L/(s·m) and 0.00014 ~ 0.083 L/(s·m), respectively, which belong to the medium category. The old empty water is due to the goaf formed after the mining of the upper horizontal coal seam, collapse crack and other filling channels accept the recharge of atmospheric precipitation, surface water and groundwater, resulting in water accumulation in the low-lying area of the goaf, which is the main source of water filling in the mine. According to the principle of high or low, the hydrogeological type of Daliuta well is divided into medium type.

The coal seam of Daliuta coal mine(Chen, 2016; Chen et al., 2016) is shallow, mainly 2^{-2} coal seam and 5^{-2} coal seam. The buried depth of 2^{-2} coal seam in mining area is 30.6 ~ 133.3 m, the recoverable area is 73.1 km^2, the average coal seam thickness is 4.37 m, at present ,2^{-2} coal seam has been mined. At present ,2^{-2} coal seam has been mined and divided into 5 disc areas, Among them, Sipan District (goaf of 22400–22405 working face), Lao Liupan District (goaf of 22601–22607 working face) and Xin Liupan District (goaf of 22608–22616 working face) have built underground reservoirs of No .1, 2 and 3 respectively. The water storage situation of underground reservoir in Daliuta Coal Mine is detailed in Table 1 (Song et al., 2020).

Table 1
Water storage and usage information of underground reservoir

Underground reservoir	No .1	No .2	No .3
Average reservoir depth (m)	7.9	5.8	8.3
Area of goaf (km^2)	3.81	1.82	2.23
Dynamic water ($\times10^4$ m^3)	165	89	153.8
Static water ($\times10^4$ m^3)	171.2	103.5	27.99
Maximum water storage capacity ($\times10^4$ m^3)	617.3 (h = 10m)	339.2 (h = 16m)	633.5 (h = 14m)
Sewage recharge (m^3/d)	9.78×10^3		
Underground water reuse (m^3/h)	330		
Surface water consumption (m^3/d)	4.5×10^3		
Total water storage ($\times10^4$ m^3)	710.5		

The buried depth of 5^{-2} coal seam in the second level is 162.9 ~ 280.0 m, and the main mining area of Daliuta Mine is 5^{-2} coal Sanpan area. The goaf formed after mining of 5^{-2} coal seam has built two water recycling chambers, and the No .4 underground reservoir is under construction. There are three kinds of water sources in underground reservoirs, including the water content of each underground water-bearing rock group, the entering goaf along the fissure zone formed by coal mining, and underground production sewage injected into goaf by drainage pipe (Song et al., 2020). Coal mine water mainly contains suspended matter, Fe, Mn, organic matter and oil and other pollutants, which are produced by natural and human factors (Mhlongo et al., 2018; Qin et al., 2006; Rathi et al., 2017).

3. Materials And Methods

3.1 Sample collection

On the basis of the field conditions of Daliuta coal mine in the study area, the site water samples of the coal mine underground reservoir located in the 2^{-2} coal seam were collected at the No .1 reservoir 400 outlet (S4) and 406 outlet (S5), No .2 reservoir recharge facilities (S2) and outlet (S6), No .3 reservoir inlet (S3) and outlet (S7). The mine water samples (S1) and the fissure water samples (S8) were collected in the water recycling chamber and the side waterway of coal mining face in the 5^{-2} coal seam respectively. The sampling scheme design and technology were strictly carried out in accordance with the industry industry standard "Technical guidance for Water quality sampling" (HJ 494–2009) and "Technical Design of Water quality sampling Scheme" (HJ 495–2009) implementation.

Since it was impossible to collect the rock samples from three coal mine underground reservoirs in 2^{-2} coal seam, this study collected roof caving rock samples from 5^{-2} coal seam mining face with similar characteristics for analyzing the characteristics of element composition, mineral composition, surface morphology, specific surface area/pore structure of rock in reservoir.

3.2 Test method of rock sample analysis

The collected rock samples and filtered suspended matter in mine water were ground to the particle size that could pass through 200 mesh sieve. Shimadzu (XRF-1800) Japanese Neo-Confucianism (ZSX Primus Ⅱ) X-ray fluorescence spectrometer was used for qualitative and semi-quantitative analysis of elements. Using a SmartLab SE type X-ray diffractometer (XRD) (Cu target, Kα radiation, step size of 0.02°, power of 40 kV, 150 mA, continuous scanning) produced by Rigaku Corporation of Japan for mineral composition analysis, test conditions: 2^{θ} angle range was 5–80° and scanning speed was 4°/min. According to the

standard analysis method, the measured XRD data were used to determine the composition of the minerals contained in rock samples and suspended matter in mine water using the Jade 6.0 (MDI, Livermore, CA, USA) software in conjunction with the material standard powder diffraction data (PDF 2004) provided by the International Centre for Diffraction Data (ICDD). The surface morphology of the samples was observed by scanning electron microscopy (Phenom Desktop SEM) produced by Phenom-World companies in the Netherlands. The ASAP 2020M Rapid Specific Surface/Pore Analyzer (BET) was used to analyze the specific surface area, total pore volume and average pore size of the samples. The measuring range of the specific surface area of the instrument is 0.005 m^2/g to infinity, and the measuring range of pore size distribution is 0.35 to 500 nm, and the minimum detection limit of pore volume analysis is 0.0001 cc/g (using H-K or DA analysis method).

3.3 Water sample analysis test method

Referring to the method of "groundwater quality inspection method" (DZ/T 0064-1993), the physical indexes such as chroma and visible matter of water sample were observed and recorded in the field. The pH value and electrical conductivity (EC) of water sample were measured immediately using handheld analyzing kits after the field collection. Some of the water samples were filtered through a 0.45 μm membrane filter and loaded into a polyethylene container. The collected samples were kept on ice in the dark and transported to laboratory as soon as possible for further analysis. The concentration of suspended solids (SS) and total soluble solids (TDS) were determined by gravimetric method. Because of the low content of suspended matter in the effluent and fissure water of the collected reservoir, the turbidity of the effluent water sample and the fissure water sample was tested by turbidimeter. Determination of chemical oxygen demand (COD) by rapid digestion spectrophotometry. The concentration of total organic carbon (TOC) was measured by a total organic carbon analyzer (TOC-LCPH CN200, Shimadzu, Japan), ultraviolet absorbance at 254 nm (UV_{254}) tested with 752 UV-Vis spectrophotometer. CO_3^{2-} and HCO_3^- concentration were determined by double mixed indicator titration. The concentration of Cl^- and SO_4^{2-} were determined by ion chromatograph (IC), and the chromatographic conditions were as follows: leaching solution concentration (sodium carbonate 0.0018 mol/L - Sodium bicarbonate 0.0017 mol/L), 25 μL injection volume, the flow rate of leaching solution was 1.0 ~ 2.0 mL/min, regenerated liquid was determined according to the flow rate of leaching solution. The concentration of K^+, Na^+, Ca^{2+}, Mg^{2+}, total heavy metals (THM) and dissolved heavy metals (DHM) were determined by PerkinElmer NexION 300D inductively coupled plasma mass spec-trometry (ICP-MS) (United States). Total heavy metal (THM) concentration refers to the concentration of heavy metal ions filtered by 0.45 μm membrane filter after acidification and digestion in mine water. The concentration of dissolved heavy metal (DHM) refers to the concentration of heavy metal ions in mine water filtered directly by 0.45 μm membrane filter without acidification and digestion. The concentration of heavy metal ions in suspended matter (SHM) was the total heavy metal concentration (THM) minus the dissolved heavy metal concentration (DHM). Each water quality index was repeatedly tested more than three times, and the average value was calculated for subsequent analysis.

3.4 PHREEQC - based reverse hydrogeochemical simulation

In order to analyze the type of water-rock interaction occurring in coal mine underground reservoirs, the reverse geochemical simulation of water-rock interaction in coal mine underground reservoirs with different paths was conducted using the INVERSE-MODELING module of PHREEQC software. The principle of reverse geochemical simulations was based on the mass conservation model (Shabani and Zivar, 2020), namely the composition and content of chemicals in final water downstream of the same path, through a series of water-rock interaction such as precipitation, dissolution, ion exchange, mixing and evaporation occurring during the water flow, which reach equilibrium with the substances in the upstream initial water, and infer the possible geochemical action in the path. In this study, selected each reservoir inlet water sample as the initial water and outlet water sample as the final water. That was, the reverse simulation operation of coal mine underground reservoir in four paths: Path I (S1→S4), Path II (S1→S5), Path III (S2→S6) and Path IV (S3→S7).

The reliability of hydrogeochemical simulation results mainly depended on the selection of the possible mineral phase and the determination of constraint variables (Dai and Samper, 2006). According to the XRF, XRD and SEM test results of the roof rock samples, the water chemical composition of the water samples and the storage conditions of the water in the underground reservoir, Quartz, Calcite, Dolomite, Gypsum, Halite, Albite, Orthoclase, Kaolinite, Illite, Chlorite, CO_2, NaX-CaX_2 cation exchange were selected as the possible mineral phases in the model. Some "possible mineral phase" and its reaction equations were shown in Table 2 (Shabani and Zivar, 2020; Zhang et al., 2020). Selected the K, Ca, Na, Mg, Cl, C, S and Si eight elements and pH value as the constraint variables in the model.

Table 2
Possible mineral phases and reaction equations

Composition	Chemical formula	Reaction equation
Albite	$NaAlSi_3O_8$	$NaAlSi_3O_8 + 8H_2O = Na^+ + Al(OH)_4^- + 3H_4SiO_4$
Orthoclase	$KAlSi_3O_9$	$KAlSi_3O_9 + 8H_2O = K^+ + Al(OH)_4^- + 3H_4SiO_4$
Dolomite	$CaMg(CO_3)_2$	$CaMg(CO_3)_2 = Ca^{2+} + Mg^{2+} + 2CO_3^{2-}$
Gypsum	$CaSO_4{\cdot}H_2O$	$CaSO_4{\cdot}H_2O = Ca^{2+} + SO_4^{2-} + 2H_2O$
Halite	NaCl	$NaCl = Na^+ + Cl^-$
Calcite	$CaCO_3$	$CaCO_3 = Ca^{2+} + CO_3^{2-}$
Cation exchange	CaX_2, NaX, MgX_2, KX	$Ca \leftrightarrow 2Na \leftrightarrow Mg \leftrightarrow 2K$
CO_2 (g)	CO_2 (g)	$CO_2 + H_2O = H_2CO_3^0$

4. Results And Discussion

4.1 Characterization of suspended matter and roof rock sample

4.1.1 Chemical and mineral composition analysis

By using the XRF, the spectral semi-quantitative mineral element composition analysis results of suspended matter in mine water and roof rock sample were detailed in Table 3. The main elements of suspended matter in mine water was C, its oxide CO_2 ratio was 91.63%, followed by SiO_2, Al_2O_3 and CaO, and contained a small amount of other elements. The proportion of SiO_2 and Al_2O_3, content in roof rock samples was 78.7%, followed by K, Na, Ca, Mg, C, S, Cl, and a small amount of other elements such as Fe, Mn, Ti, etc. It showed that the main mineral composition in the roof rock sample was meta-aluminate or silicate (Fang et al., 2020).

Table 3
The chemical composition of suspended matter and roof rock sample (%)

Composition	CO_2	Na_2O	MgO	Al_2O_3	SiO_2	P_2O_5	SO_3	Cl	K_2O	CaO
Roof rock	8.6352	1.0352	1.2241	19.1005	59.614	0.2059	0.0597	0.0138	3.5551	0.4485
Suspended matter	91.6334	0.1213	0.1224	1.8917	2.9136	0.0222	0.2086	0.2347	0.1193	1.9888
Composition	TiO_2	CdO	Cr_2O_3	MnO	Fe_2O_3	Co_2O_3	NiO	CuO	ZnO	Ga_2O_3
Roof rock	0.8929	—	0.0131	0.0383	5.0591	0.0022	0.0057	0.0049	0.0261	0.0028
Suspended matter	0.0499	0.007	0.0019	0.018	0.6198	—	0.0005	0.0005	0.0166	—
Composition	As_2O_3	Rb_2O	SrO	Y_2O_3	ZrO_2	Nb_2O_5	Br			
Roof rock	—	0.0125	0.0167	0.003	0.0282	0.0027	—			
Suspended matter	0.0007	0.0014	0.0104	—	—	—	0.0174			
Note: "—" means no or no detection.										

The mineral composition in suspended matter and roof rock sample was qualitatively and semi-quantitatively analyzed by XRD. The results were shown in Fig. 1. The minerals of suspended matter in mine water were mainly graphite, accounting for 73.8%, followed by calcite (11.8%), kaolinite (9.2%) and quartz (5.2%). The higher calcite may be due to the direct drying without deionized filtration during the pretreatment of suspended matter, which made the Ca^{2+} react with CO_3^{2-} or the CO_2 in air dissolved in mine water to form calcite. The main minerals in roof rock samples included quartz, feldspar and clay minerals. The order of percentage of mineral components was Quartz (43.7%) > Albite (15.9%) > Kaolinite (12.4%) > Alurgite (9.9%) > Chlorite (7.9%) > Orthoclase (6.9%) > Illite (2.8%) > Muscovite (0.5%). There may be a certain amount of Gypsum, Halite, Calcite, Dolomite, Pyrite and other coal seam symbiotic minerals in the roof rock sample. The analysis showed that the Mg elements in the roof rock samples were mainly from chlorite, some of which may also came from dolomite or other minerals; K elements were mainly from orthoclase, Illite and mica minerals; Na elements were mainly from albite, some may also come from mica minerals; Ca elements were mainly from calcite, dolomite and other impurity minerals. Some studies have shown that minerals containing K, Na, Ca, Mg, S and other elements may participate in water-rock interaction, and affect the concentration of ions in water (Chander et al., 2020; Tao et al., 2007). The XRD analysis results showed that the mineral composition and content of suspended matter and roof rock sample were basically consistent with the results of XRF element analysis.

4.1.2 Surface morphology and specific surface area/pore structure analysis

The collected rock samples and suspended matter in mine water were observed by scanning electron microscope, and the surface morphology scanning results were as shown in Fig. 2. The layered silicate structure and flake kaolinite structure can be clearly seen on the rock sample surface of coal seam roof, and there were thin and strip shapes with irregular size and shape, as well as some irregular microcracks (as shown in Fig. 2(a)). When rocks interact with mine water, these edges and cracks may adsorb some ions in mine water (Pearce et al., 2018). The particles of roof rocks in underground reservoir of coal mine were arranged closely and the particle gradation was good. According to the engineering practice and the analysis results of water sample data on the spot, the roof rocks had a good filtration effect on mine water. Figure 2(b) of suspended matter in mine water showed that there were a large number of other substances adsorbed on graphite surface, and the carbon molecules in pulverized coal had organic reducibility, which can make suspended matter in mine water adsorbed COD and other soluble substances (Jiang et al., 2020; Zhang et al., 2021).

The specific surface area of rock minerals can characterize the adsorption properties of substances, and the specific surface area and pore structure of collected rock samples and suspended matter in mine water were listed in Table 4. The specific surface area of roof rock samples was 7.7323 ~ 9.7297 m^2/g, the average value was 8.6548 m^2/g; the suspended matter was 9.103 ~ 11.9089 m^2/g, and the average value was 10.1065 m^2/g. The mean of total pore volume of roof rock samples was 0.02687 cc/g, and the suspended matter was 0.03842 cc/g. It can be seen that the specific surface area and total pore volume of roof rock samples were lower than those of suspended matter in mine water. The higher specific surface area and total pore volume were more favorable for the adsorption and removal of ions or pollutants in mine water. The adsorption capacity of suspended matter in mine water was higher than that in roof rock samples. XRF analysis and surface morphology analysis of suspended matter in mine water showed that other substances were attached to the

surface of suspended matter, which indicated that the settlement of suspended matter had a certain purification effect on other pollutants in mine water. The measured pore size of roof rock samples was 8.6108 ~ 13.732 nm, the average was 11.8978 nm; the suspended matter was 9.6024 ~ 16.808 nm, the average was 14.5454 nm. The pore size of suspended matter in mine water was larger than that of roof rock sample, which indicated that the pore distribution in suspended matter was more dense. The samples were classified according to the pore size classification standard proposed by the International Federation of Pure and Applied Chemistry (IUPAC). It can be seen that the field rock samples and mine water suspensions belong to mesoporous materials (2 ~ 50 nm) (Zhang et al., 2020).

Table 4
Surface structure and pore distribution of suspended matter and roof rock sample

Sample	Specific surface area (m^2/g)				Total pore volume (cc/g)			Average pore diameter (nm)			
	BET	Langmuir	BJH Adsorption	BJH Desorption	Single point	BJH Adsorption	BJH Desorption	BET Adsorption	BET Desorption	BJH Adsorption	BJH Desorption
Roof rock	8.30	9.73	7.73	8.86	0.027	0.027	0.027	13.07	8.61	13.73	12.17
Suspended matter	9.41	11.91	9.10	10.00	0.039	0.038	0.038	16.44	9.60	16.81	15.33

4.2 Hydrochemical characteristics analysis of water samples

The physiochemical characteristics of the inlet and outlet water were summarized in Table 5. The water samples from underground reservoir in this area were slightly alkaline and EC was 1627 ~ 1937 us/cm, characterized the concentration of soluble salt in the solution, belong to fresh water (TDS < 1000 mg/L) (Zhang et al., 2021). The average value of inlet TDS concentration of underground reservoir was 937 mg/L, and the average value of effluent was 866 mg/L. The average value of influent of SS concentration was 1231 mg/L, the average turbidity of effluent was 98.5 NTU. The average value of inlet COD was 51.87, and the average value of effluent was 30.17. TOC and UV_{254} can be used to characterize the DOM fractions (Zheng et al., 2015). The mean TOC and UV_{254} concentrations of influent water samples were 0.163 mg/L and 14.69 cm^{-1}, effluent concentrations were 0.021 mg/L and 10.54 cm^{-1}, respectively. It can be seen that the pollutant concentration of TDS, suspended material and COD, dissolved organic matter from the reservoir water decreased.

Table 5
Physiochemical characteristics of mine water

Sample	pH	EC (us/cm)	TDS (mg/L)	SS (mg/L)	Turbidity (NTU)	COD	UV_{254} (cm^{-1})	TOC (mg/L)
S1	7.15	1801	901	2496	—	60.85	0.175	16.41
S2	7.05	1937	976	560	—	38.42	0.161	13.91
S3	7.06	1920	934	636	—	56.34	0.152	13.75
S4	7.15	1720	904	—	99	30.27	0.027	8.84
S5	7.09	1627	814	—	98.5	35.30	0.015	13.28
S6	7.04	1723	869	—	98.5	28.67	0.014	8.25
S7	8.22	1757	878	—	98	26.45	0.027	11.80
S8	7.15	1756	837	—	78	25.32	0.011	7.37
Note: "—" means no detection.								

The concentration of Fe and Mn in each sample and the percentage of its existence were shown in Fig. 3, and the concentration of other heavy metal ions were less than 0.01 mg/L, such as copper, zinc and chromium and so on. The average concentration of Fe-DHM in the influent was 0.053 mg/L, the average concentration of Fe-SHM was 9.79 mg/L, and the proportion of Fe-DHM and Fe-SHM was 0.51% and 99.49% respectively. The average concentration of Fe-DHM in effluent was 0.315 mg/L, the average concentration of Fe-SHM was 0.75 mg/L, and the proportion was 29.25% and 70.75%, respectively. The average concentrations of Mn-DHM and Mn-SHM in the inlet water of the reservoir were 0.107 mg/L and 0.577 mg/L, with a percentage of 14.71% and 85.29%, respectively. The average concentrations of Mn-DHM and Mn-SHM in reservoir effluent were 0.032 mg/L and 0.142 mg/L, with a percentage of 18.86% and 81.14%, respectively. The concentration of Fe-DHM and Mn-DHM in the effluent of the reservoir was higher than that in the influent. The analysis may be that the iron and manganese ions adsorbed on the suspended matter were desorbed into the water phase or the minerals containing Fe and Mn in the underground reservoir of the coal mine dissolved (Jiang et al., 2020).

The reservoir water sample analysis showed that the roof collapse rock in the underground reservoir in the coal mine had a certain purification effect on the mine water, and the effluent water quality was significantly improved. The concentration of pollutants in water samples (S1) collected in water circulation chamber of 5^{-2} coal seam was higher than that of influent (S2 and S3) of underground reservoir in 2^{-2} coal seam. The collected S1 water sample was kept static for a period of time, and most of the suspended objects in the water sample were settled to the bottom of the container. Combined with the

characteristic analysis results of suspended matter in mine water. It was shown that the sedimentation of suspended matter occurs in the water circulation chamber of 5^{-2} coal seam, which made the suspended matter in mine water be removed to a certain extent, and the adsorption of suspended matter surface also reduced the dissolved pollutants in mine water. Therefore, in order to improve the pollutant purification effect and service life of the coal mine underground reservoir, the pollutants deposited at the bottom of the 5^{-2} coal bed water circulation chamber shall be removed in time. The pollutant indexes of fracturing water sample (S8) in underground reservoir were lower than that of inlet and outlet water samples of the reservoir, and the reservoir effluent water samples were close to S8 water quality, indicating that the mixed effect of upper fissure water and mine water improved the effluent water quality of the reservoir.

4.3 Analysis of the variation of hydrochemical types and major ions of water samples

To intuitively compare the size differences between the ion concentrations of water samples collected in each field. The Schoeller diagram (Al-Barakah et al., 2017) was drawn with 3 groups of main cations (Na^++K^+, Ca^{2+}, Mg^{2+}) and anions (Cl^-, SO_4^{2-} and HCO_3^-+CO_3^{2-}) as the transverse coordinates, with the mole concentration and the ion valence product value (meq/L or meq/kg) as longitudinal coordinates, as shown in Fig. 4. Field water samples mainly contained Na^+, Ca^{2+}, SO_4^{2-} and Cl^-, and less content of Mg^{2+} and HCO_3^-. The Na^+ and Cl^- content in the effluent of the reservoir increased and the Ca^{2+}, Mg^{2+} and SO_4^{2-} content decreased compared with the concentration of each ion in the influent of the reservoir. The concentration of each ion in the fissure water was similar to that in the reservoir effluent, which indicated that the mixture of mine water and fissure water occurs in the underground reservoir of coal mine. The interaction between water and rock may occurred between the influent and rock of the reservoir, which made the ion concentration of the effluent change.

A tri-linear diagram of the Piper by the percentage of the molar concentration of each major anion and the valence product of ionization (Shan et al., 2019; Sun and Gui, 2012), as shown in Fig. 5. According to the difference of the distribution area from the sample point to the diamond map, the hydrochemical type of the water sample can be directly reflected. Piper diagram results showed that the main hydrochemical types of mine water in the field were the SO_4^{2-}-Cl^-/Ca^{2+}, and the hydrochemical types of reservoir effluent mainly included SO_4^{2-}-Cl^-/Na^+ and SO_4^{2-}-Cl^-/Ca^{2+}. The main hydrochemical types of inlet and outlet water were 36-A type (SO_4^{2-}-Cl^-/Ca^{2+}) and 42-A type (SO_4^{2-}-Cl^-/Na^+) according toucarev numbering method, which was consistent with the results of Piper three-line graph analysis. This transition from the main ion concentration and hydrochemical types indicated that mine water interacts with rocks during storage and migration of underground reservoirs in coal mines (Han et al., 2020a).

In order to determine the main water-rock interactions occurring and the source of ions in the effluent of underground reservoir in coal mine. Three scatter diagrams were plotted (Fig. 6) by ion ratio method. The main sources of Na^+ during water-rock interaction can be analyzed by the ion ratio method of Na^+ and Cl^-, as shown in Fig. 6a. Three reservoir inlet water samples (Cl^-, Na^+) scatter are all below on the line of y = x (Bozau et al., 2017). The molar concentration ratio of Na^+ and Cl^- of S2 and S3 water samples were greater than that of 1, then the Na^+ content was higher than that of Cl^-, and the Na^+ and Cl^- concentration ratio of the effluent water sample of No .1 reservoir was larger than that of the influent water sample. The results showed that the dissolution of Na^+ occurred in the coal mine underground reservoir and mainly from silicate minerals like sodium feldspar was consistent with the mineral composition analysis of rock.

As shown in Fig. 6b, the inlet water samples (Ca^{2+}+Mg^{2+}) vs. (SO_4^{2-}+HCO_3^-) scatter were distributed along the line y = x (Ettazarini, 2005), while all outlet water all points were above the ratio line. It can be seen that the water-rock interaction deficient the concentration of (Ca^{2+}+Mg^{2+}) of reservoir relative to (SO_4^{2-} +HCO_3^-). One of the reasons for the Na^+ excess and (Ca^{2+}+Mg^{2+}) deficiency may be a cation exchange reaction, thus causing the release of Na in the rock and reducing the concentrations of Ca^{2+} and Mg^{2+} in the water. The farther the (Na^+-Cl^-) vs. (Ca^{2+}+Mg^{2+}- SO_4^{2-}-HCO_3^-) plot distance of the line of y=-x indicating strong cation exchange (Zhang et al., 2019). Figure 6c showed that each water sample point in the influent was farther away from the y = x line than the sample point in the effluent. The results showed that the cation exchange reaction occurred in coal mine underground reservoir, which made the Na^+ in the rock was replaced by Ca^{2+} and Mg^{2+} in the water, and the cation exchange ability of the effluent water samples weaken (Zhang et al., 2019).

4.4 Reverse hydrogeochemical simulation results of water-rock interaction in coal mine underground reservoir

The water-rock mass balance reaction model of coal mine underground reservoir under different paths was shown in Fig. 7. Positive value indicated that the mineral phase was dissolved, the ions or elements entered into the mixed water; the negative value indicated that the mineral phase settled in the mixed water and the ions leaved the mixed water; "zero" meant that no reaction had occurred (Salcedo Sánchez et al., 2017). The simulation results of Path I (Fig. 7a) showed that Orthoclase, Albite, Halite and Dolomite dissolved 0.039 mmol/L, 0.17 mmol/L, 1.7 mmol/L and 0.53 mmol/L respectively, while Gypsum, Kaolinite, Quartz and Calcite precipitated 0.46 mmol/L, 0.10 mmol/L, 0.41 mmol/L and 1.2 mmol/L respectively; Illite did not take part in the reaction. Path II (Fig. 7b) simulation results showed that Halite and Albite dissolved 1.6 mmol/L and 0.18 mmol/L respectively; Quartz, Calcite, Gypsum and Kaolinite precipitated 0.35 mmol/L, 0.15 mmol/L, 0.48 mmol/L and 0.089 mmol/L respectively; Illite, Orthoclase and Dolomite did not participate in the reaction. Path III (Fig. 7c) simulation results showed that Halite and Albite dissolved 0.28 mmol/L and 0.11 mmol/L respectively; Quartz, Calcite, Dolomite, Gypsum and Kaolinite precipitated 0.21 mmol/L, 0.085 mmol/L, 0.0049 mmol/L, 0.80 mmol/L and 0.053 mmol/L respectively; and cation exchange occurred (NaX: 2.83; CaX_2: -1.42), Orthoclase and Illite did not participate in the reaction. Path IV (Fig. 7d) simulation results showed that Calcite, Halite and Albite dissolved 0.49 mmol/L, 0.34 mmol/L and 1.15 mmol/L respectively, and carbon dioxide gas dissolved 0.48 mmol/L; Quartz, Dolomite, Gypsum and Kaolinite precipitated 2.3 mmol/L, 0.57 mmol/L, 0.15 mmol/L and 0.58 mmol/L respectively, and cation exchange occurred (NaX: 1.94; CaX_2: -0.97), Orthoclase and Illite did not take part in the reaction.

According to the above analysis results, the dissolution of Albite and Halite, the precipitation of Gypsum and the replacement of Na^+ in rock by Ca^{2+} in the water mainly occurred in the underground reservoir of coal mine, resulting in the increased of Na^+ and Cl^- concentration and the decreased of Ca^{2+} and SO_4^{2-} concentration in the outlet water, and the hydrochemical type changes from type SO_4^{2-}-Cl^-/Ca^{2+} to type SO_4^{2-}-Cl^-/Na^+. Little or no dissolution of Orthoclase and Illite resulted in little change of K^+ concentration in the effluent water. The dissolution or precipitation behavior of Calcite and Dolomite in rocks with different paths was inconsistent, which was mainly related to ionic strength in water, content in rocks and environmental conditions (Salcedo Sánchez et al., 2017). At the same time, the dissolution of carbon dioxide and the precipitation of Quartz and Kaolinite may occurred in the reservoir. The simulation results of PHREEQC software were consistent with the analysis results of rock mineral composition and ion ratio, and more detailed information of water-rock interaction was obtained, which indicated that the hydrogeochemical reverse simulation software can be effectively used to analyze the water-rock interaction in underground reservoir of coal mine.

5. Conclusions

This study implied that the main mineral composition of roof caving rock samples in underground reservoir was metaaluminate or silicate. The layered silicate structure and flaky kaolinite structure can be clearly visible on the surface of the rock, with some irregular edges and micro cracks, and the collapsed rock had a higher specific surface area and total pore volume. These characteristics made the collapse rocks in the reservoir had a certain adsorption and removal capacity for suspended solids, COD, DOM, heavy metal ions and other pollutants in the mine water, and have a certain purification effect on the mine water. In addition, the high content of graphite in the suspended solids in the mine water can absorb other dissolved pollutants in the water, and the mixing effect of overlying fissure water and mine water in the reservoir also made the water quality of the reservoir effluent water improved significantly. The water rock interaction between the collapsed rock and the mine water, such as the dissolution of albite and halite, the precipitation of gypsum, quartz and kaolinite, and the cation exchange reaction, resulted in the increase of the concentration of Na^+ and Cl^- and the decrease of the concentration of Ca^{2+}, Mg^{2+} and TDS in the reservoir outlet water, and the hydrochemical type changed from SO_4^{2-}-Cl^-/Ca^{2+} type to SO_4^{2-}-Cl^-/Na^+ type. The simulation results of PHREEQC software were consistent with the analysis results of rock mineral composition and ion ratio method, and more detailed information of water rock interaction can be obtained. It showed that the hydrogeochemical reverse simulation software can be effectively used to analyze the water rock interaction in underground reservoir of coal mine.

6. Declarations

Ethics approval and consent to participate: Not applicable

Consent for publication: Not applicable

Availability of data and materials: All data generated or analysed during this study are included in this published article.

Competing interests: The authors declare that they have no competing interests.

Funding and Acknowledgements: This work was co-supported by the scientific and technological innovation project of Shenhua Group (SHJT-16-28), the science and technology project of Shendong company in 2020 (202016000041), the Fundamental Research Funds for the Central Universities (2021YJSHH19), the Yue Qi Young Scholar Project, China University of Mining & Technology, Beijing (2019QN08), and the Research on Ecological Restoration and Protection of Coal Base in Arid Eco-fragile Region (GJNY2030XDXM-19-03.2).

Authors' contributions: BJ and JG involved in samples testing, data analysis and manuscript writing in this study, and they were major contributor in writing the manuscript. KD tested and analyzed the characteristics of the reservoir water samples. XD tested and analyzed the characterization of the rock samples. KZ involved in data analysis and manuscript writing. All authors read and approved the final manuscript.

7. References

1. Al-Barakah, F.N., Al-jassas, A.M. and Aly, A.A. 2017. Water quality assessment and hydrochemical characterization of Zamzam groundwater, Saudi Arabia. Applied Water Science 7(7), 3985-3996.
2. Bozau, E., Licha, T. and Ließmann, W. 2017. Hydrogeochemical characteristics of mine water in the Harz Mountains, Germany. Geochemistry 77(4), 614-624.
3. Chander, V., Tewari, D., Negi, V., Singh, R., Upadhyaya, K. and Aleya, L. 2020. Structural characterization of Himalayan black rock salt by SEM, XRD and in-vitro antioxidant activity. Sci Total Environ 748, 141269.
4. Chandrasekhar, S., Sharma, H. and Mohanty, K.K. 2018. Dependence of wettability on brine composition in high temperature carbonate rocks. Fuel 225(AUG.1), 573-587.
5. Chen, S. (2016) Research on the Key Technology of Water Resources Recycling Utilization in the Underground Goaf Reservoir in Shendong Mining Area. Doctoral dissertation, Xi'an University of Science and Technology.
6. Chen, S., Huang, Q., Xue, G. and Li, R. 2016. Technology of underground reservoir construction and water resource utilization in Daliuta Coal Mine. Coal Science and Technology 44(08), 21-28.
7. Dai, Z. and Samper, J. 2006. Inverse modeling of water flow and multicomponent reactive transport in coastal aquifer systems. Journal of Hydrology 327(3-4), 447-461.

8. Embile, R.F., Walder, I.F. and Mahoney, J.J. 2019. Multicomponent reactive transport modeling of effluent chemistry using locally obtained mineral dissolution rates of forsterite and pyrrhotite from a mine tailings deposit. Advances in Water Resources 128(JUN.), 87-96.
9. Ettazarini, S. 2005. Processes of water–rock interaction in the Turonian aquifer of Oum Er-Rabia Basin, Morocco. Environmental Geology 49(2), 293-299.
10. Fang, M., Li, X., Zhang, G., Liu, Q., Tuo, K. and Liu, S. 2020. Discussion on water-rock interaction mechanism in underground reservoir of Daliuta coal mine. Coal Science and Technology, 1-8.
11. Fang, Z. (2020) Research on Mechanism of Purifying Underground Reservoir Water Storage by Collapsed Coal Rock in Goaf of Wanli No.1 Coal Mine. Master's thesis, China University of Mining and Technology.
12. Goren, O., Gavrieli, I., Burg, A. and Lazar, B. 2011. Cation exchange and CaCO3 dissolution during artificial recharge of effluent to a calcareous sandstone aquifer. Journal of Hydrology 400(1-2), 165-175.
13. Gu, D. 2015. Theory framework and technological system of coal mine underground reservoir. Journal of China Coal Society 40(02), 239-246.
14. Gu, D., Li, T., Li, J., Guo, Q., Jiang, B., Bian, W. and Yixiang, B. 2021. Current status and prospects of coal mine water treatment technology in China. Coal Science and Technology 49(01), 11-18.
15. Gu, D., Zhang, Y. and Cao, Z. 2016. Technical progress of water resource protection and utilization by coal mining in China. Coal Science and Technology 44(01), 1-7.
16. Han, J., Gao, J., Du, K., Chen, M., Jiang, B. and Zhang, k. 2020a. Analysis of hydrochemical characteristics and formation mechanism in coal mine underground reservoir. Coal Science and Technology 48(11), 223-231.
17. Han, J., Yu, y., Zheng, R., Li, M., Zhang, K. and Jiang, B. 2020b. Analysis of the source of DOM in underground reservoir of coal mine. Journal of Mining Science and Technology 5(05), 575-583.
18. Hidalgo, M.C. and Cruz-Sanjulián, J. 2001. Groundwater composition, hydrochemical evolution and mass transfer in a regional detrital aquifer (Baza basin, southern Spain). Applied Geochemistry 16(7-8), 745-758.
19. Ibrahim, R.G.M., Korany, E.A., Tempel, R.N. and Gomaa, M.A. 2019. Processes of water–rock interactions and their impacts upon the groundwater composition in Assiut area, Egypt: Applications of hydrogeochemical and multivariate analysis. Journal of African Earth Sciences 149, 72-83.
20. Jannesar Malakooti, S., Shahhosseini, M., Doulati Ardejani, F., Ziaeddin Shafaei Tonkaboni, S. and Noaparast, M. 2015. Hydrochemical characterisation of water quality in the Sarcheshmeh copper complex, SE Iran. Environmental Earth Sciences 74(4), 3171-3190.
21. Jia, H., Qian, H., Zheng, L., Feng, W., Wang, H. and Gao, Y. 2020. Alterations to groundwater chemistry due to modern water transfer for irrigation over decades. Sci Total Environ 717, 137170.
22. Jiang, B., Liu, S., Ren, J., Zheng, R., Chen, M., Yu, y. and Zhang, K. 2020. Purification effect of coal mine groundwater reservoir on mine water containing organic compounds and heavy metals in different occurrence forms. Coal Engineering 52(01), 122-127.
23. Korrani, A., Sepehrnoori, K. and Delshad, M. 2015. Coupling IPhreeqc with UTCHEM to model reactive flow and transport. Computers & geosciences 82(sep.), 152-169.
24. Kumar, P., Mahajan, A.K. and Kumar, A. 2020. Groundwater geochemical facie: implications of rock-water interaction at the Chamba city (HP), northwest Himalaya, India. Environ Sci Pollut Res Int 27(9), 9012-9026.
25. Li, Z., Wang, G., Wang, X., Wan, L., Shi, Z., Wanke, H., Uugulu, S. and Uahengo, C.-I. 2018. Groundwater quality and associated hydrogeochemical processes in Northwest Namibia. Journal of Geochemical Exploration 186, 202-214.
26. Ma, L., Du, X., Wang, F. and Liang, J. 2013. Water-preserved Mining Technology for Shallow Buried Coal Seam in Ecologically-vulnerable Coal field: A case study in the Shendong Coal field of China. Disaster Advances 6, 268-278.
27. Mahani, H., Keya, A.L., Berg, S. and Nasralla, R. 2016. Electrokinetics of Carbonate/Brine Interface in Low-Salinity Waterflooding: Effect of Brine Salinity, Composition, Rock Type, and pH on ?-Potential and a Surface-Complexation Model. SPE Journal 22(01), 53-68.
28. Mhlongo, S.p., Mativenga, P.T. and Marnewick, A. 2018. Water quality in a mining and water-stressed region. Journal of Cleaner Production 171, 446-456.
29. Pearce, J.K., Turner, L. and Pandey, D. 2018. Experimental and predicted geochemical shale-water reactions: Roseneath and Murteree shales of the Cooper Basin. International Journal of Coal Geology 187, 30-44.
30. Phan, T.T., Paukert Vankeuren, A.N. and Hakala, J.A. 2018. Role of water–rock interaction in the geochemical evolution of Marcellus Shale produced waters. International Journal of Coal Geology 191, 95-111.
31. Qin, F., Wen, B., Shan, X.Q., Xie, Y.N., Liu, T., Zhang, S.Z. and Khan, S.U. 2006. Mechanisms of competitive adsorption of Pb, Cu, and Cd on peat. Environ Pollut 144(2), 669-680.
32. Rathi, B., Siade, A.J., Donn, M.J., Helm, L., Morris, R., Davis, J.A., Berg, M. and Prommer, H. 2017. Multiscale Characterization and Quantification of Arsenic Mobilization and Attenuation During Injection of Treated Coal Seam Gas Coproduced Water into Deep Aquifers. Water Resources Research 53(12), 10779-10801.
33. Salcedo Sánchez, E.R., Garrido Hoyos, S.E., Esteller, M.V., Martínez Morales, M. and Ocampo Astudillo, A. 2017. Hydrogeochemistry and water-rock interactions in the urban area of Puebla Valley aquifer (Mexico). Journal of Geochemical Exploration 181, 219-235.
34. Shabani, A. and Zivar, D. 2020. Detailed analysis of the brine-rock interactions during low salinity water injection by a coupled geochemical-transport model. Chemical Geology 537.
35. Shan, Y., Wang, W., Qin, Y. and Gao, L. 2019. Multivariate analysis of trace elements leaching from coal and host rock. Groundwater for Sustainable Development 8, 402-412.

36. Shao, L. (2009) Study on the Technology for in Situ Treatment and Utilization of Underground Mine Water. Doctoral dissertation, China University of Mining & Technology,Beijing.
37. Sharma, H. and Mohanty, K.K. 2018. An experimental and modeling study to investigate brine-rock interactions during low salinity water flooding in carbonates - ScienceDirect. Journal of Petroleum Science and Engineering 165, 1021-1039.
38. Shi, X. 2021. Research progress and prospect of underground mines in coal mines. Coal Science and Technology, 1-10.
39. Song, H., Xu, J., Fang, J., Cao, Z., Yang, L. and Li, T. 2020. Potential for mine water disposal in coal seam goaf: Investigation of storage coefficients in the Shendong mining area. Journal of Cleaner Production 244.
40. Sprocati, R., Masi, M., Muniruzzaman, M. and Rolle, M. 2019. Modeling electrokinetic transport and biogeochemical reactions in porous media: A multidimensional Nernst-Planck-Poisson approach with PHREEQC coupling. Advances in Water Resources 127(MAY), 134-147.
41. Steding, S., Zirkler, A. and Kühn, M. 2020. Geochemical reaction models quantify the composition of transition zones between brine occurrence and unaffected salt rock. Chemical Geology 532.
42. Sun, L.H. and Gui, H.R. 2012. Chemistry of Groundwater from Two Aquifers in Liuyi Coal Mine, Northern Anhui Province, China: a Comparative Study. Applied Mechanics and Materials 212-213, 362-365.
43. Tao, S., Bi-wan, X. and Hui-sheng, S. 2007. The evolution of coal gangue (CG)–calcium hydroxide (CH)–gypsum–H2O system. Materials and Structures 41(7), 1307-1314.
44. Wang, Q., Li, W., Li, T., Li, X. and Liu, S. 2018. Goaf water storage and utilization in arid regions of northwest China: A case study of Shennan coal mine district. Journal of Cleaner Production 202, 33-44.
45. Yu, Y., Chen, W., Cao, Z., Chen, J. and Zhang, K. 2018. Research on change features on dissolved organic matter of mine water in coal mine's underground reservoir. China Coal 44(10), 168-173.
46. Zhang, D., Fan, G., Ma, L. and Wang, X. 2011. Aquifer protection during longwall mining of shallow coal seams: A case study in the Shendong Coalfield of China. International Journal of Coal Geology 86(2-3), 190-196.
47. Zhang, K., Gao, J., Jiang, B., Han, J. and Chen, M. 2019. Experimental study on the mechanism of water-rock interaction in the coal mine underground reservoir. Journal of China Coal Society 44(12), 3760-3772.
48. Zhang, K., Gao, J., Men, D., Zhao, X. and Wu, S. 2021. Insight into the heavy metal binding properties of dissolved organic matter in mine water affected by water-rock interaction of coal seam goaf. Chemosphere 265, 129134.
49. Zhang, K., Li, H., Han, J., Jiang, B. and Gao, J. 2020. Understanding of mineral change mechanisms in coal mine groundwater reservoir and their influences on effluent water quality: a experimental study. International Journal of Coal Science & Technology 8(1), 154-167.
50. Zheng, L., Song, Z., Meng, P. and Fang, Z. 2015. Seasonal characterization and identification of dissolved organic matter (DOM) in the Pearl River, China. Environmental Science and Pollution Research 23(8), 7462-7469.

Figures

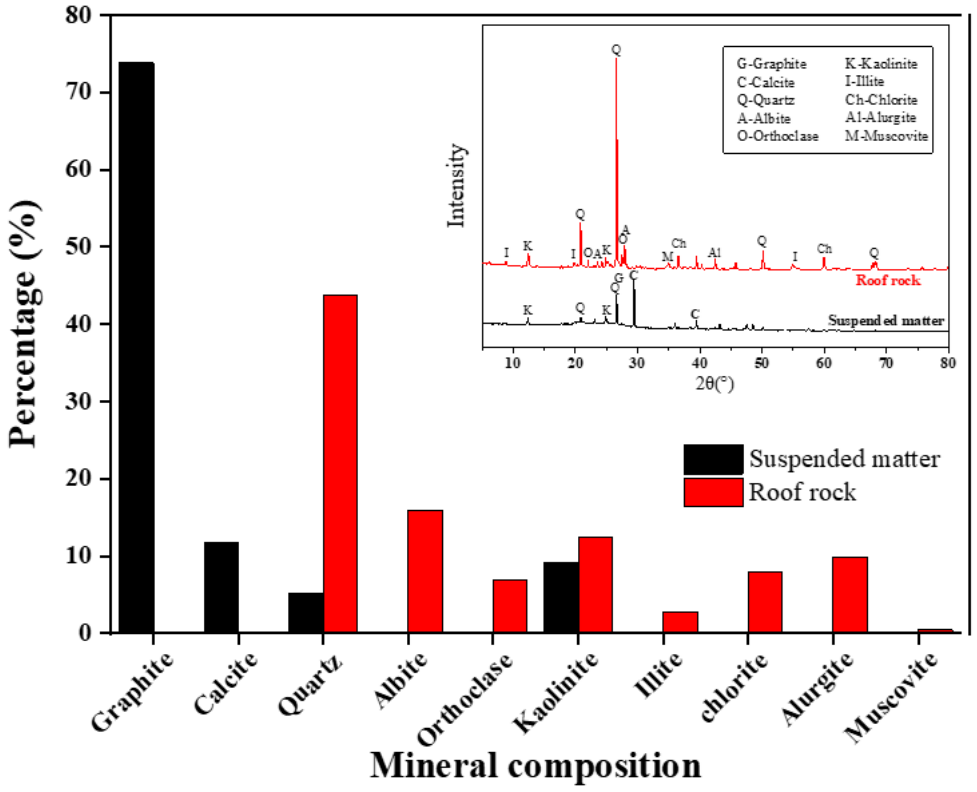

Figure 1

Analysis of mineral composition of suspended matter and roof rock sample

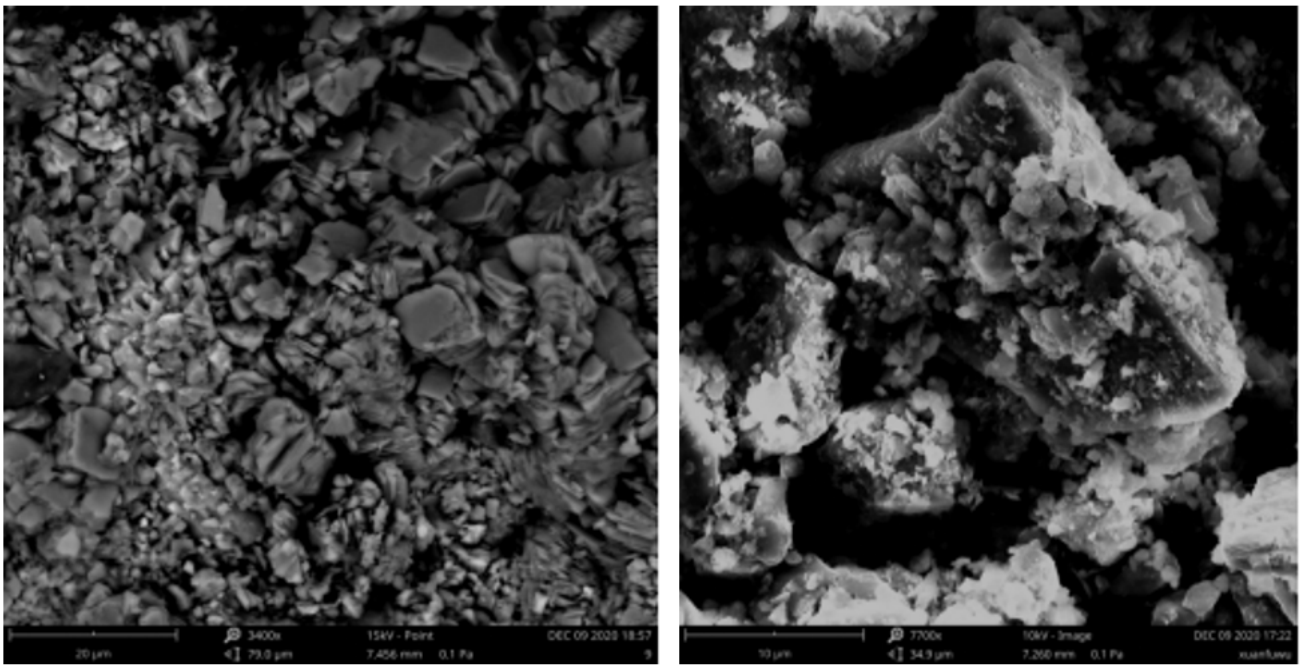

(a) Roof rock sample (b) Suspended matter

Figure 2

SEM morphology of roof rock sample and suspended matter in mine water

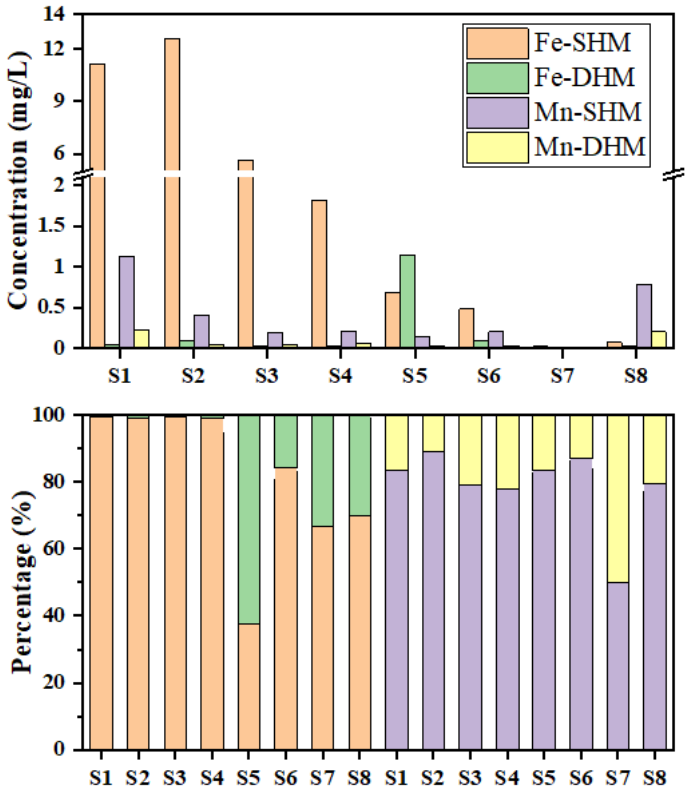

Figure 3

Concentration of Fe and Mn in water samples and percentage of its present forms at each sampling point. SHM: heavy metal ions in suspended matter; DHM: the dissolved heavy metal concentration.

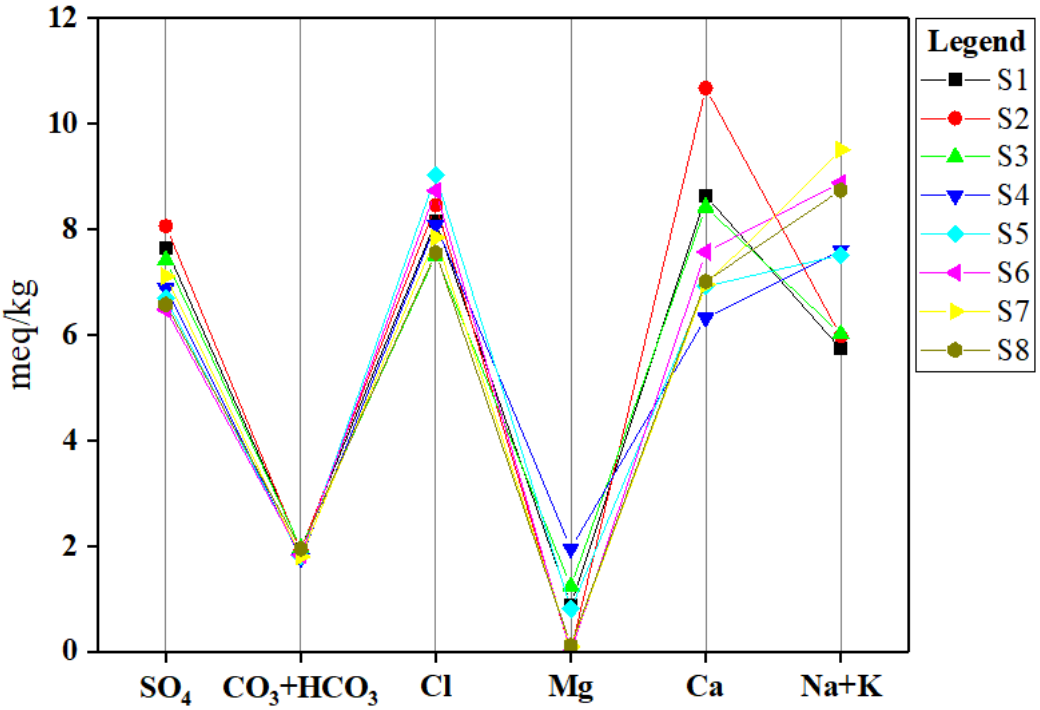

Figure 4

Schoeller diagram indicating ionic concentrations of water samples in the study area.

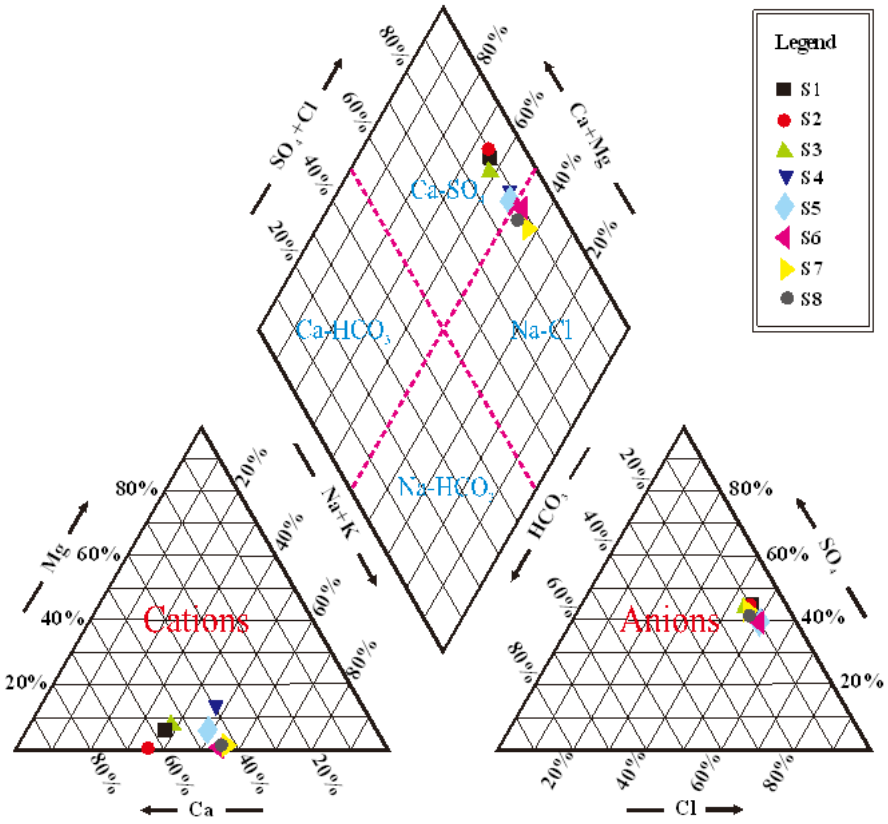

Figure 5

Piper tri-linear diagram of water samples on site.

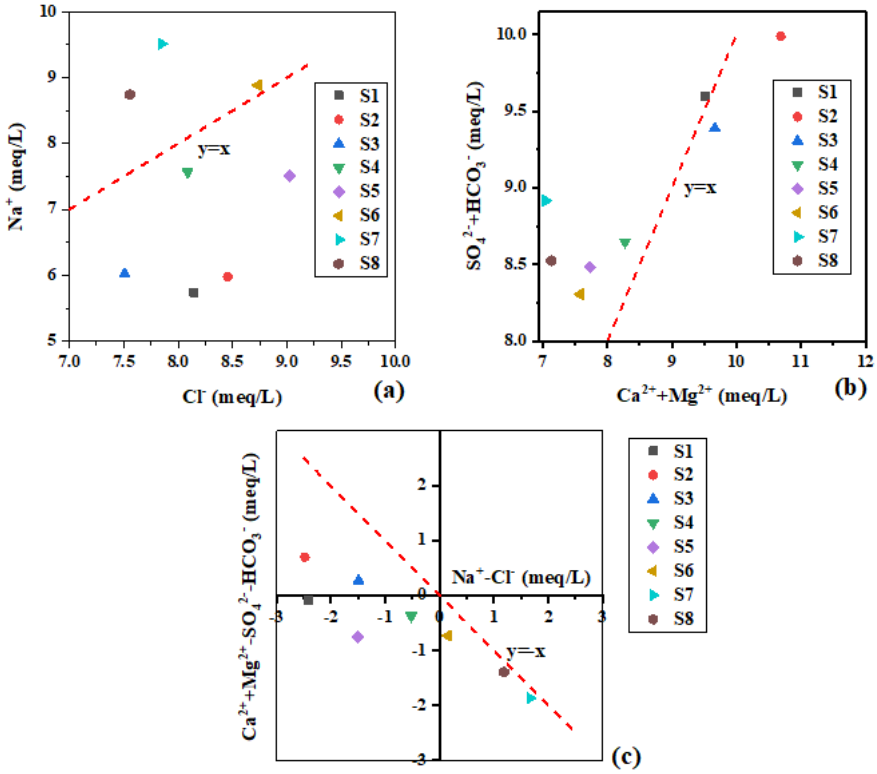

Figure 6

Scatter diagram of compositions of water samples in the study area. (a) Cl- vs. Na+; (b) Ca2++Mg2+ vs. SO42-+HCO3-; (c) Na+-Cl- vs. Ca2++Mg2+- SO42–HCO3-.

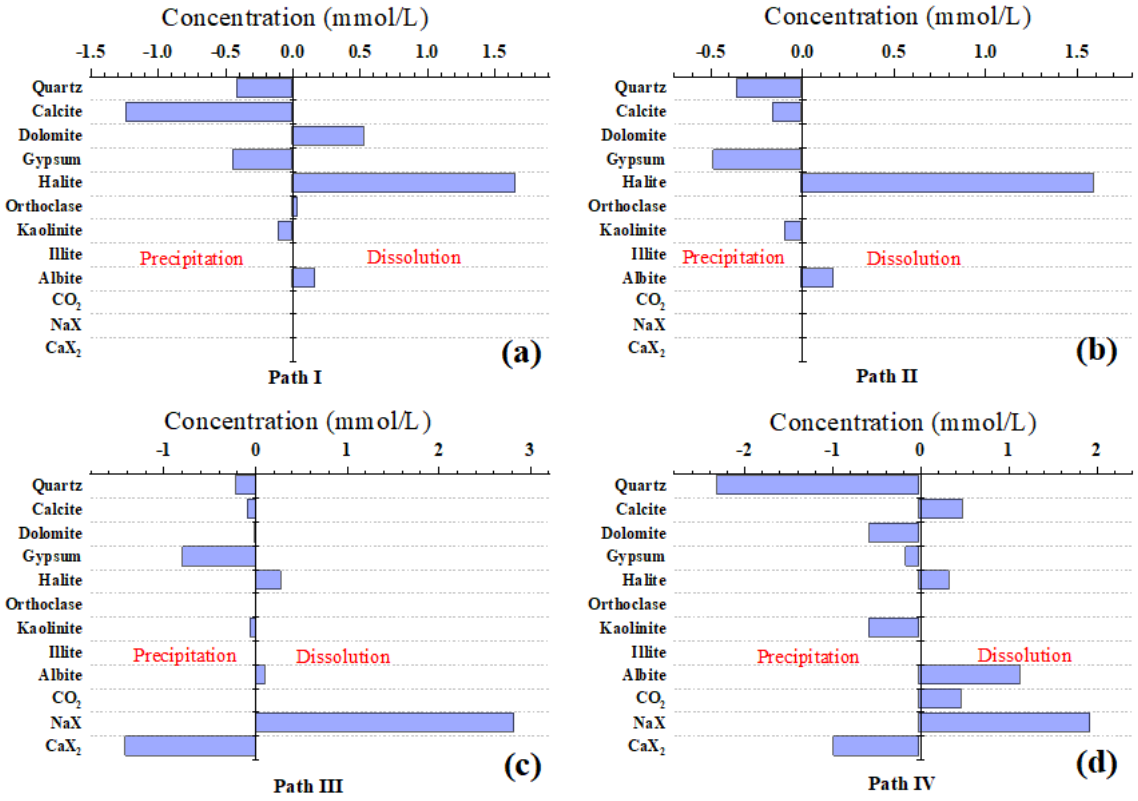

Figure 7

Mass balance reaction models of water-rock interaction of four paths of coal mine underground reservoir.